Available online at www.sciencedirect.com

ScienceDirect

Procedia Manufacturing 38 (2019) 108–116

Procedia MANUFACTURING

www.elsevier.com/locate/procedia

29th International Conference on Flexible Automation and Intelligent Manufacturing (FAIM2019), June 24-28, 2019, Limerick, Ireland

Dynamic Predictive Modeling of Solder Paste Volume with Real Time Memory Update in a Stencil Printing Process

Hongya Lu, Haifeng Wang, Sang Won Yoon, Daehan Won, and Seungbae Park

Department of Systems Science and Industrial Engineering, State University of New York at Binghamton
Binghamton, NY 13905, U.S.A

Abstract

This research aims to develop a dynamic prediction model to assist real-time decision making of a stencil printing process by maintaining high prediction accuracy of the printing process. In a Surface Mount Technology (SMT) assembly line, the stencil printing process (SPP) accounts for more than 50% of the defectiveness of printed circuit boards (PCBs). During the printing process, environmental changes such as humidity or wear of blades may induce the PCBs printing results to deviate from the target volume. Thus, real-time adjustment of the printer settings (e.g., printing parameters, clean cycles, etc.) based on prediction of printing volumes is critical to maintain a high printing performance. However, research has been limited in real time SPP control, which is partially due to the difficulties in predicting the paste volumes with high accuracy and time efficiency. To tackle the challenges, this research proposes novel online learning models for real-time SPP status prediction. The prediction model is implemented by selecting advanced online learning models to estimate the printing volumes in averages and standard deviations (SDs) considering different pad sizes with different clean ages, directions, printer parameters, etc. The model performances are evaluated in Root Mean Square Error ($RMSE$), R^2, etc. From comparison, the Support Vector Regressor (SVR) shows outstanding prediction performance with R^2 values of 92% and 81% for volume averages and SDs. This research emphasizes the potential of using online learning as a preliminary process for effective real-scenario SMT assembly dynamic control.

Keywords: Solder paste stencil printing; support vector regression; online sequential extreme learning machine; online learning; Surface Mount Technology

1. Introduction

Surface mounting is a technology to attach electronic components to a printed circuit board (PCB). In a surface mount technology (SMT) based assembly (Figure 1), stencil printing process (SPP) is a critical procedure which controls deposition of solder paste to the PCB. The SPP accounts for 60% of soldering

2351-9789
10.1016/j.promfg.2020.01.015

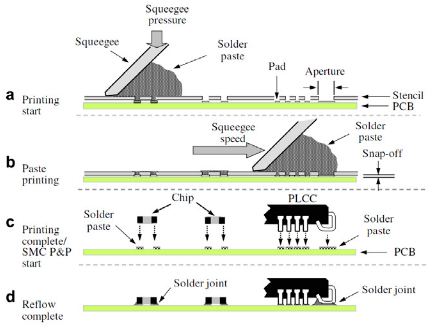

Fig. 1. A typical surface mount assembly [4].

defects in the PCB assembly [1], and it is considered as a key affecting the first-pass-yields of PCBs. The quality of solder paste printing process, which is related to the PCB yield rates, is normally interpreted from the printed solder paste volumes detected during the Stencil Printing Inspection (SPI) process, which functions to control the SPP settings. Basically, influential factors on the solder paste volumes include the clean cycle, direction, squeegee parameters, environmental conditions, and printer settings [2]. As described in Figure 1, critical printer settings include squeegee speed, squeegee pressure and separation speed. Printer settings are controllable factors to enhance the SPP performance, and optimal settings of such parameters have been studied in recent research. Unconstrained optimization models have been formulated to obtain optimal printer settings [3], operation levels on squeegee and snap-off height [4], etc. Such optimization models have been based on prediction modeling of the printer system status by analyzing relationships between printing results and the influential factors. To study the causal effects, machine learning techniques have been explored by training a prediction model using experimental data acquired from the design of experiments (DOE) [3].

During the SPP, unexpected changes may happen to the printing environment in temperature, humidity, wear of components, etc. Such changes can induce a significant variation from the relationship between machine settings (e.g., cleaning cycle, printing speed) and the solder paste volumes. Hence, the estimation of machine parameter optimality based on the knowledge acquired at the start of system can deviate from the current system status. The optimal settings from the initial experience may lose the advantages, and induce the PCBs printing results to deviate from the desired results. Thus, the predictive modeling of the dynamic system status based on new incoming printing data is critical to maintain the optimality of printer settings. To solve the problem, real-time adaptation of the prediction model is an effective and cost-efficient solution. However, research has been rarely done for real-time modeling of the SPP, due to the natural variation characteristic of the SMT system. Online learning is a machine learning paradigm to update prediction functions based on real-time systems inputs, which has been intensively studied in data stream systems such as cancer prognosis [5], visual tracking [6], and credit card default [7]. With an accurate and time efficient online prediction model which maps real-time system status from relevant features, the understanding of printing system can be significantly enhanced in mass production lines. Subsequently, optimization results based on prediction estimation can be well linked to the practical system.

This research proposes online learning techniques to perform the real-time modeling of a SPP. Online prediction models are proposed to predict real-time SPP volumes averages and standard deviations (SDs) considering different pad sizes with different clean ages and printer parameters. The model performances are evaluated in root mean square error ($RMSE$), R^2, etc. This research focuses on designing two models: the Online Sequential Extreme Learning Machine (OSELM) and the offline Support Vector Regressor (SVR) which retrains with the most recent certain number of PCB data. From the comparison study, the SVR which learns from a short-term memory shows outstanding prediction effectiveness with R^2 values of 92% and 78% for the volume average and SD models. The OSELM exhibits impressive training efficiency. The proposed online learning models exhibit potential for effective dynamic control on the real-scenario SMT assembly and highlights the significance of high accuracy online learning in SPP control.

The rest of this paper is organized as follows. Section 2 presents a review of recent literature about SMT prediction modeling; Section 3 introduces the proposed methodology in this research; experimental settings and results are shown in Section 4; conclusion and future work of SMT assembly dynamic modeling is discussed in Section 5.

2. Literature Review

The SPP predictive modeling has been extensively studied in recent years by analyzing the printing results and related printing factors in an offline and static strategy. Machine or environmental factors that potentially influence the SPP performances have been sufficiently explored [3, 8]. Printing parameters including printing speed (PS), printing pressure (PP) and squeegee separation speed (SS) have been identified as critical factors to the SPP performances, and control systems based on such parameters have been investigated [9, 10]. The relationships between printing parameters and stencil printing behavior have been modeled using the Decision Tree (DT), Neural Networks (NN), and SVR [3, 4]. By using one-pass-training strategies offline and generating outstanding learning performances, such research papers validated the high correlation of parameter setting on the printing results in a PCB assembly line, where PP, PS and SS are frequently studied machine settings.

In the area of data-driven SPP control, real-time SPP modeling research has shown limited success compared to the well-developed offline SMT prediction models. The difficulties are most likely related to the complexity and natural variability of the process [11]. The preliminary structure of closed-loop real-time process control system for a PCB assembly was established in [12], which specified a fuzzy control system with corrective actions on the stencil printing parameters based on inspection feedback. Later, a comprehensive structure of a self-organizing SPP control system was proposed with software design and implementation [13]. Based on the theories, a practical closed-loop online feedback control system for the SPP was developed by using Neural Networks as the prediction model to assist real-time parameter selection [11]. The global optimization technique is used for real-time SPP parameter update as continuous variates in [14], which adopts a quadratic objective function for performance estimation. NN approaches have been studied for real-time inspection frequently in later years [15, 16]. By using the online NN for real-time volume estimation, the model in [16] achieved 5% error for sample mean and 8% for sample variance. However, the system required high memory cost, and the optimization performance was indeterminate. The real-time modeling of SPP is stilling facing challenges which traditional NNs are not sufficient to fulfill.

A real-time SPP prediction model requires high prediction accuracy and low computational burden. Real-time prediction is a critical part for dynamic control, which can influence the optimization performance and total computational time. However, most research papers focused on the optimization model instead of the prediction model, and most research used traditional NN approaches to estimate solder paste volumes [14, 16, 17]. Traditional NNs have drawbacks in generalization and convergence, and normally require massive parameter tuning work [18]. Such drawbacks may affect practical application performances. The offline SVR and DT also tend to be overfitting during the printing process, degrading the accuracy for generalization. Online learning algorithms for regression have been extensively studied in recent years to tackle challenges in generalization, convergence and training efficiency. Well-developed online regression techniques include online gradient boosting [19], online Gaussian Process Regression (OGPR) [20], online sequential extreme learning machine (OSELM) [21], etc. The OSELM is a model proposed based on traditional Extreme Learning Machines (ELM) [22], which has been validated to produce high generalization performances with low training time [21]. In addition, the offline SVR has shown promising results for generalization in the work of [3]. The long and short term memory acquired by SVR deserves to be investigated to find the most useful information that contribute to high accuracy in SVR. Thus, in addition to the OSELM, a SVR model is formulated which retrains with short term memory.

3. Methodology

The principles of OSELM and SVR are briefly introduced in this section to provide the theoretical foundation to this research.

3.1. Support Vector Regressor

The SVR technique is a regression version of the traditional Support Vector Machines, which solves a complicated nonlinear regression problem by mapping input features to a high dimensional space [3]. The SVR is summarized in this subsection by referring to the research in [23]. For a dataset with input and output $\vec{X} = \{\vec{x}_1, ..., \vec{x}_N\}$, $\vec{T} = \{T_1, ..., T_N\}$, the SVR generates an optimal separating hyperplane for $\vec{x}_i$ $(i = 0, 1)$ described as:

$$F = \omega^T \rho(\vec{x}_i) + b \tag{1}$$

where $\rho(x)$ represents a nonlinear mapping from the feature space to the high-dimensional hyperplane, ω denotes the weight vector, and b is the bias constant. The ω and b in the hyperplane can be determined from solving the quadratic programming problem:

$$\min_{\omega,b} S(\omega) = \tfrac{1}{2}\omega\omega^T + M \textstyle\sum_{i=1}^{n} \phi_i \tag{2}$$

$$s.t. \quad T_i[\omega^T \rho(\vec{x}_i) + b] \geq 1 - \phi_i \tag{3}$$

where $\phi_i > 0$ are slack variables to allow errors to exist. $M > 0$ is for regularizing the variable. The dual of the minimization problem is described as follows:

$$\max_{\gamma_i} S(\omega) = -\tfrac{1}{2} \textstyle\sum_{i,j=1}^{n} \gamma_i T_i \gamma_i T_j K(x_i \cdot x_j) + \sum_{i=1}^{n} \gamma_i \tag{4}$$

$$s.t. \qquad \textstyle\sum_{i=1}^{n} \gamma_i T_i = 0, M \geq \gamma_i \geq 0 \tag{5}$$

The α_i which corresponds to x_i is the support vector. The kernel function K needs to satisfy the Mercer condition, yielding to the optimal decision function:

$$y_i = \sum_{i=1}^{n} \gamma_i T_i K(x_i \cdot x_j) + b \tag{6}$$

The prediction result is hereby obtained by y_i.

3.2. Online Sequential Extreme Learning Machine

The OSELM on the basis of ELM was developed for Single Layer Feedforward Networks (SLFN) with additive and Radial Basis Function (RBF) hidden nodes [22]. With random feature mapping from the input to the hidden layer, and with back-propagation training by minimizing least-squared errors (LSE), the memory of the ELM stored in the output layer weight vector $\vec{\beta}$ is calculated as follows:

$$\vec{\beta} = \vec{H}^{+}\vec{T} = (\vec{H}^T\vec{H})^{-1}\vec{H}^T\vec{T} \tag{7}$$

where $\vec{T}$ is a sequence of prediction targets, and $\vec{H}$ is the output from the hidden layer. $\vec{H}^{+}$ represents the Moore-Penrose generalized inverse of matrix $\vec{H}$. Formula 7 generates the LSE solution for the ELM. The OSELM learns incrementally by updating the weight vector $\vec{\beta}$ with data streams in either single observations or chunks. At the initialization stage, the hidden layer output matrix $\vec{H}_0$ is first calculated with randomly generated input weights and the activation function. The output weight $\vec{\beta}_0$ is then estimated with $\vec{H}_0$ and the initial batch of observations. Starting from $k = 0$ at initialization, the online learning stage calculates the randomly mapped output $\vec{H}_{k+1}$ from the incoming s samples, and the corresponding update of hidden layer output is calculated in $\vec{\beta}_{k+1}$. In data chunk $k+1$, the weight matrix $\vec{\beta}_{k+1}$ is updated with a combination of $\vec{\beta}_k$ and $\vec{H}_{k+1}$. The pseudo code of the algorithm is depicted in the Algorithm 1.

Algorithm 1 OSELM Method [21]

Input: Training input and output $\vec{X} = \{\vec{x}_0, ..., \vec{x}_N\}$, $\vec{T} = \{T_1, ..., T_N\}$; R neurons; activation function f

Initialization phase:

1: Randomly generate input weight $\vec{w}_0$ and $\vec{b}_0$

2: Calculate the hidden layer output $\vec{H}_0 = f(\vec{x}_0, \vec{w}_0, \vec{b}_0)$

3: Calculate output weight vectors $\vec{\beta}_0 = \vec{H}_0{}^+ T_0$ and $\vec{P}_0 = (\vec{H}_0{}^T \vec{H}_0)^+$

Online learning phase:

4: For Batch $k+1$ with s new samples, calculate the hidden layer output $\vec{H}_{k+1} = f(\vec{x}_{k+1}, \vec{w}_k, \vec{b}_k)$

5: Calculate the output weights β_{k+1}

6: if $s > 1$ then

7: $\quad \vec{P}_{k+1} = \vec{P}_k - \vec{P}_k \vec{H}_{k+1}{}^T (\vec{I} + \vec{H}_{k+1} \vec{P}_k \vec{H}_{k+1}{}^T)^{-1} \vec{H}_{k+1} \vec{P}_k$

8: $\quad \vec{\beta}_{k+1} = \vec{\beta}_k - \vec{P}_{k+1} \vec{H}_{k+1}{}^T (\vec{T}_{k+1} - \vec{H}_{k+1} \vec{\beta}_k)$

9: else

10: $\quad \vec{P}_{k+1} = \vec{P}_k - \frac{\vec{P}_k \vec{H}_{k+1} \vec{H}_{k+1}{}^T \vec{P}_k}{1 + \vec{H}_{k+1}{}^T \vec{P}_k H_{k+1}}$

11: $\quad \vec{\beta}_{k+1} = \vec{\beta}_k + \vec{P}_{k+1} \vec{H}_{k+1} (T_{k+1} - \vec{H}_{k+1}{}^T \vec{\beta}_k)$

12: end if

13: Output: $Y_{k+1} = \vec{H}_{k+1} \vec{\beta}_{k+1}$

4. Experimental Results

Details of data acquisition and predictive modeling results have been presented and discussed.

4.1. Experimental Settings

A localized Surface Mount Assembly, which consists of a stencil printer and a SPI machine, was built in the laboratory to estimate the SPI prediction accuracy. A testing board is printed repetitively with real-time inspection data iteratively generated. The printer settings are controlled in terms of printing speed, printing pressure and squeegee separation speed. For the system setup, the initial setting for real-time printing has been generated based on a DOE with 20 combinations of PS, PP, and SS. In the dynamic printing process, 4 boards are printed as a batch. At the end of each batch, real-time inspection data are collected and the optimal setting is updated. The experiment runs 10 batches recursively by printing 40 boards for each model. Two dynamic models are compared: 1) online learning with OSELM; 2) offline learning by retraining a SVR model at each batch, with a training set combining the most recent 20 boards and the 20 DOE boards. The system information has been indicated in Table 1 with the testing PCB information and machine settings. The selection of squeegee size is based on the PCB size. To avoid defects induced by infrequent cleaning or excessive strokes, a short cleaning cycle and a single stroke printing strategy are used.

Table 1. System information of both SVR and OSELM based experiments.

Factor	Specifications
Printer Settings	Printing Speed, Printing Pressure, Separation Speed
Pad Sizes	Area Ratio, Aspect Ratio
Printing Direction	forward & backward, single stroke
Pad Types / Board	26
No. of Pads / Board	3141
Squeegee	300 mm blade
Cleaning Cycle	2 (vacuum dry)
Other	room temperature & humidity

4.2. Performance Evaluation

During the printing process, the dynamically updated OSELM and SVR models are tested with the next batch after training. For each of the batch (e.g., batch i), the data obtained at batch $i+1$ are used as testing datasets to assess the prediction performance of either OSELM or SVR. The OSELM is updated in an online manner, which renews the model parameters whenever data from batch i are received by the model. To eliminate the retraining time, a total of 40 boards are used to retrain SVR at each iteration. The SVR is retrained according to 20 DOE boards data and the latest 20 boards in dynamic printing. The DOE data which are less inclined to induce noise assist the model to gain basic system information, and the dynamic data allows the SVR model to learn from real-time system status. The boards used for training SVR is indicated in Table 2.

Table 2. Number of PCBs included as short-term memory for training a SVR model.

Batch	1	2	3	4	5	6	7	8	9	10
Add Previous Online Batches	0	1	2	3	4	4	4	4	4	4
DOE Boards	20	20	20	20	20	20	20	20	20	20
Total Boards for Training	24	28	32	36	40	40	40	40	40	40

Two prediction models are trained separately during the printing process: volume averages ($Vol.Avg$) and volume SDs ($Vol.SD$). For each of the method, the two models are estimated and compared. The performances of two models are compared in perspectives of RMSE, Mean Absolute Error, R^2 and normalized RMSE. In addition, the fitness of distributions between the target and the prediction results are compared and assessed at different stages of printing.

4.3. Results Analysis

The dynamic prediction results using OSELM and SVR are presented in Figure 2, and the numerical results for the $RMSE$ and R^2 are shown in Table 3. For a general comparison, the SVR with short-term memory update shows significantly higher values in R^2 fitness, and lower values in $RMSE$, MAE, $NRMSE$ for both $Vol.Avg$ and $Vol.SD$ models. OSELM updates at each batch upon arrival of new data. From the significantly reducing trend of error, OSELM is shown to be learning effectively. However, the accuracy is lower than SVR, potentially due to the simplicity of single layer OSELM. The SVR slowly removes old data since Batch 6. With offline training with recent data, SVR turns out to be stable and accurate, with slightly decreasing errors during learning. Until the end of experiment, the SVR generates $RMSE = 3.28$ and $R^2 = 0.92$ for $Vol.Avg$; $RMSE = 0.85$ and $R^2 = 0.81$ for $Vol.SD$. Such results indicate that SVR with short-term memory update has effectively acquired dynamic system status information.

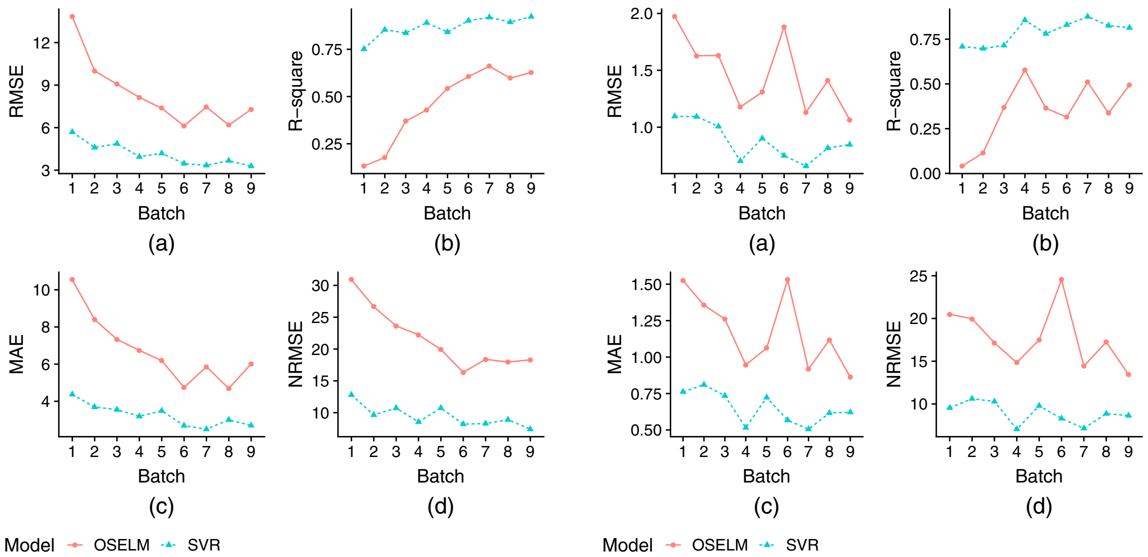

(1) $Vol.Avg$ model accuracy.

(2) $Vol.SD$ model accuracy.

Fig. 2. Prediction accuracy results for (1) $Vol.Avg$ and (2) $Vol.SD$ by comparing OSELM and SVR. In each subfigure, four metrics are shown. (a): RMSE; (b): R^2; (c): MAE; (d): NRMSE.

In addition to the accuracy analysis, the fitness of prediction during different batches of learning has been investigated to analyze the adaptiveness of SVR and OSELM. Figure 3 shows the fitness of SVR

Table 3. Evaluation results for $RMSE$ and R^2 from the volume average ($Vol.Avg$) and SD ($Vol.SD$) models.

Performance Metric	Prediction Model	# of Batch 1	2	3	4	5	6	7	8	9
$RMSE_{Vol.Avg}$	OSELM	13.84	10.00	9.06	8.14	7.37	6.12	7.46	6.18	7.29
	SVR	5.69	4.60	4.86	3.94	4.19	3.46	3.34	3.67	3.28
$RMSE_{Vol.SD}$	OSELM	1.97	1.63	1.63	1.18	1.31	1.88	1.13	1.41	1.06
	SVR	1.10	1.09	1.01	0.70	0.90	0.75	0.66	0.82	0.85
$R^2_{Vol.Avg}$	OSELM	0.13	0.18	0.37	0.43	0.54	0.61	0.66	0.60	0.63
	SVR	0.75	0.85	0.84	0.89	0.84	0.90	0.92	0.89	0.92
$R^2_{Vol.SD}$	OSELM	0.04	0.12	0.37	0.58	0.36	0.31	0.51	0.34	0.49
	SVR	0.71	0.70	0.72	0.86	0.78	0.83	0.88	0.83	0.81

and OSELM between prediction values and their corresponding testing targets in batches 2, 4 to 9 in a time sequential manner, with both $Vol.Avg$ and $Vol.SD$ results present in each column of the figure. In terms of the $Vol.Avg$ values, testing targets of both SVR and OSELM follow a binormal distribution, with a high peak around $Volume = 100$ and low peak around $Volume = 70$. In terms of the $Vol.SD$, both SVR and OSLEM printing results follow a single peak distribution with highest frequency of $Vol.SD$ within $[1.5, 2]$. Such consistencies indicate the intrinsic characteristics of the PCB volumes distribution by pad. For the SVR model, the prediction values distribution shows the same binormal distribution from the start of learning (Batch 2), and remains consistent through Batch 4 until Batch 9. The distribution line adjusted itself slightly and locally to fit the target line during learning, and Batch 9 shows a best fitness among previous batches. Even though SVR deletes old data from Batch 6, the capability and stability of learning has been maintained by establishing a new SVR model each iteration with latest data. With new data used to update the currently model, OSELM based distributions are comparatively improving more significantly. From Batch 2, the $Vol.Avg$ model of OSELM shows a single peak distribution, which is underfitting the binormal distribution; the $Vol.SD$ of OSELM predicted values also shows significant differences to the target values. The OSELM continuous improves, and shows the binormal distribution at Batch 4, with $Vol.SD$ also getting closer to the target. Until Batch 9, the OSELM significantly adjusted the distribution line shapes, and became closest to the target. However, as observed from Figure 3 (3)&(6), the SVR still outperforms OSELM in approximating the target distributions until Batch 9. Thus, the SVR shows a better fitness to the target, whereas the improvement by time does not appear to be significant. The OSELM significantly improves the model by learning from new datasets, while the model needs to be further enhanced for higher fitting capability.

5. Conclusion

This research aims to model the real-time characteristic of a SPP by focusing on developing dynamic prediction models for the first time. Effective learning has been achieved while continuously updating the model according to its latest status by studying online learning techniques for real-time prediction of the printer line status. A typical online learning model OSELM and a SVR retraining using short-term memory update have been proposed. To validate and compare the performances of the proposed techniques, two identical experiments using OSELM and SVR as prediction models are developed. From the comprehensive comparison in training accuracy and fitness, the SVR model shows the best overall performance, highlighting the potential of real-time learning based SPP control.

In perspective of the learning accuracy, the prediction models have been evaluated in $RMSE$, MAE, R^2 and $NRMSE$. The SVR significantly outperforms the OSELM in prediction accuracy by showing statistically higher values in R^2 and lower values in $RMSE$, etc. during the learning process. At the ending batch of learning, the SVR achieves $RMSE = 0.92$ for volume averages prediction model and $RMSE = 0.81$ for volume SDs prediction model. in perspective of the distributional fitness at each of the 10 stages of the learning process, the SVR shows remarkable goodness of fit since the start of learning, while maintaining the same line shape with slight improvements during the learning process. The OSELM exhibits high adaptiveness to adjust itself to continuously fit the target distribution. However, the goodness of fit by OSELM needs to be further enhanced. In comparison, the SVR remains invariant during the learning process in both model accuracies and fitness. Even though the OSELM shows significant improvements during the learning process,

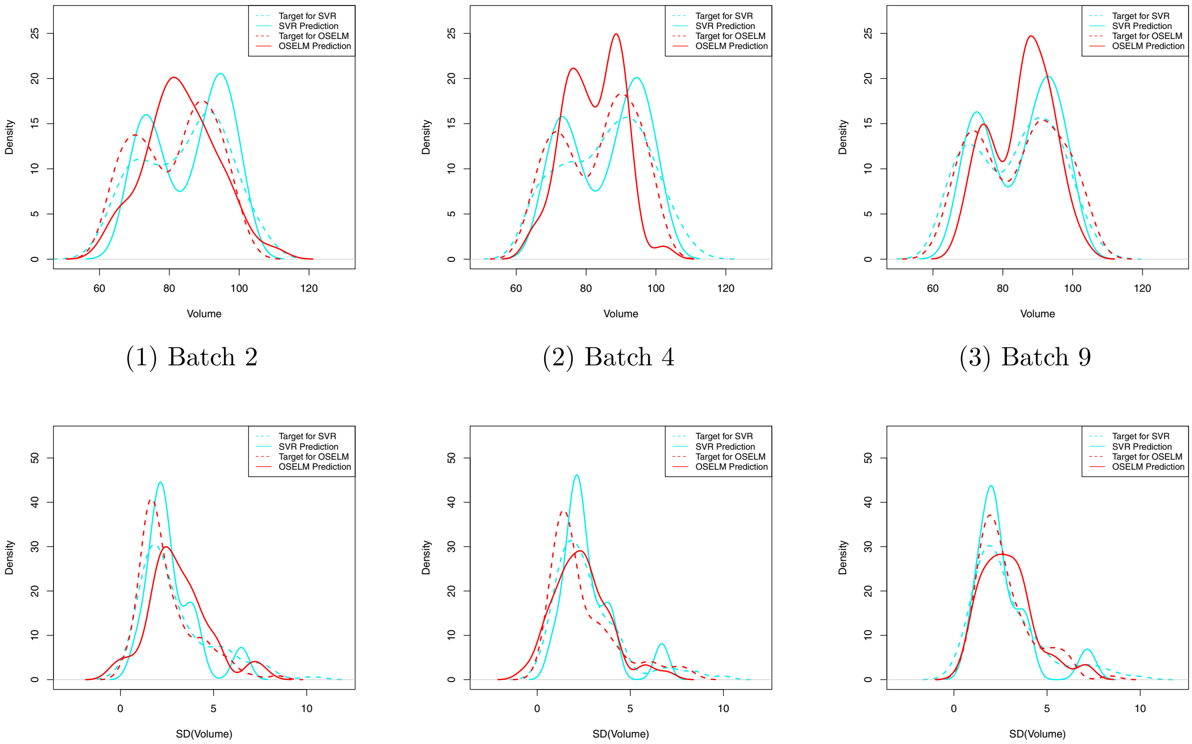

(1) Batch 2 (2) Batch 4 (3) Batch 9

(4) Batch 2 (5) Batch 4 (6) Batch 9

Fig. 3. Distributions of predicted and target results from each model at different stages of learning. (1) (2) (3) are *Vol.Avg* models, (4) (5) (6) are *Vol.SD* models.

both the accuracy and model fitness have remained significantly lower than the SVR. Therefore, the SVR which retrains with DOE data and the most recent 20 boards is validated to be effective in dynamic SPP system performance prediction.

As future work of this research, using SVR to retrain with short-term memory can be potentially degraded in performance, since noise can be included in the real-time data from the SMT production line. Detecting changes in real-time data and improving the robustness of algorithms in presence of noise and concept drifts is a critical topic to maintain high performance in SPP dynamic predictive modeling. The problem can be potentially solved by combining the online learning algorithms to noise filtering or adaptiveness enhancing techniques.

References

[1] Tennyson, N., Budiman, S., Rajkumar, D., Solomon, R., Ekere, N.N., Currie, M. A., 2000. Understanding the process window for printing lead-free solder pastes. In 50th Electronic Components & Technology Conference Proceedings. pp. 1426-1435.

[2] Wang, H., He, T., Yoon, S.W., Recurrent Neural Network-based stencil cleaning cycle predictive modeling. Procedia Manufacturing 17, 86-93.

[3] Khader, N., Yoon, S. W., 2018. Stencil printing process optimization to control solder paste volume transfer efficiency. IEEE Transactions on Components, Packaging and Manufacturing Technology 8(9), 1686-1694.

[4] Tsai, T. N., 2008, Modeling and optimization of stencil printing operations: a comparison study. Computers & Industrial Engineering 54(3), 374-389.

[5] Lu, H., Wang H., Yoon, S. W., 2019, A dynamic gradient boosting machine using genetic optimizer for practical breast cancer prognosis. Expert Systems with Applications 116, 340-350.

[6] Xu, C., Tao, W., Meng, Z., Feng Z., 2015. Robust visual tracking via online multiple instance learning with Fisher information. Pattern Recognition 48(12), 3917-3926.

[7] Lu, H., Wang H., Yoon, S. W., 2017, Real time credit card default classification using adaptive boosting-based online learning algorithm. In IIE Annual Conference Proceedings. pp. 422-427.

[8] Lotfi, A., Howarth, M., 1998. Industrial application of fuzzy systems; adaptive fuzzy control of solder paste stencil printing. Information Sciences 107(14), 273-285.

[9] Haslehurst, L., Ekere, N. N., 1996. Parameter interactions in stencil printing of solder paste. Journal of Electronics Manufacturing 6(4), 307–316.

[10] Durairaj, R., Nguty, T. A., Ekere, N. N., 2001. Critical factors affecting paste flow during the stencil printing of solder paste. Soldering & Surface Mount Technology 13(2), 30–34.

[11] Barajas, L., Kamen, E., Goldstein, A., 2001. On-line enhancement of the stencil printing process. Circuits Assembly 12(3), 32-37.

[12] Feldmann, K., Sturm, J., 1994. Closed loop quality control in printed circuit assembly. IEEE Transactions on Components, Packaging, and Manufacturing Technology: Part A 17(2), 270-276.

[13] Venkateswaran, S., Srihari, K., Adriance, J. H., Westby, G. R., 1997. A realtime process control system for solder paste stencil printing. In Electronics Manufacturing Technology Symposium, Twenty-First IEEE/CPMT International. pp. 62-67.

[14] Barajas, L., Kamen, E., Goldstein, A., Egerstedt, M., Small, B., 2002. A closed-loop control algorithm for stencil printing. In Proceedings of the Surface Mount Technology Association International Conference SMTA02. pp. 51-58.

[15] Pham-Van-Diep, G., Aravamudhan, S., Andres, F., 2003. Real time visualization and prediction of solder paste flow in the circuit board print operation. Journal of SMT 16(1).

[16] Wu, H., Zhang, X., Kuang, Y., Lu, S., 2008. A real-time machine vision system for solder paste inspection. In Advanced Intelligent Mechatronics, AIM 2008, IEEE/ASME International Conference on. pp. 205-210.

[17] Barajas, L. G., Egerstedt, M. B., Kamen, E. W., Goldstein, A., 2008. Stencil printing process modeling and control using statistical neural networks. IEEE Transactions on Electronics Packaging Manufacturing 31(1), 9-18.

[18] Zhang, J. R., Zhang, J., Lok, T. M., Lyu, M. R., 2002. A hybrid particle swarm optimization–back-propagation algorithm for feedforward neural network training. Applied Mathematics and Computation 185(2), 1026-1037.

[19] Beygelzimer, A., Hazan, E., Kale, S., Luo, H., 2015. Online gradient boosting. In Advances in Neural Information Processing Systems. pp. 2458-2466.

[20] Wang, Y., Brubaker, M. A., Chaib-draa, B., Urtasun, R., 2014. Bayesian filtering with online Gaussian process latent variable models. In UAI. pp. 849-857.

[21] Liang, N. Y., Huang, G. B., Saratchandran, P., Sundararajan, N., 2006. A fast and accurate online sequential learning algorithm for feedforward networks. IEEE Transactions on Neural Networks 17(6), 1411-1423.

[22] Huang, G. B., Zhu, Q. Y., Siew, C. K., 2006. Extreme learning machine: theory and applications. Neurocomputing 70, 489-501.

[23] Drucker, H., Burges, C. J., Kaufman, L., Smola, A. J., Vapnik, V., 1997. Support vector regression machines. In Advances in Neural Information Processing Systems, 155-161.